Transient PP2A SIP complex localization to mitotic SPBs for SIN inhibition is mediated solely by the Csc1 FHA domain

Alaina H. Willet, Liping Ren, Lesley A. Turner, and Kathleen L. Gould*
Department of Cell and Developmental Biology, Vanderbilt University School of Medicine, Nashville, TN 37240

ABSTRACT **Many organisms utilize an actin- and myosin-based cytokinetic ring (CR) to help complete cytokinesis. In *Schizosaccharomyces pombe*, the Septation Initiation Network (SIN) promotes proper CR function and stability. The SIN is a conserved and essential signaling network consisting of a GTPase and a cascade of kinases assembled at the spindle pole body (SPB). The PP2A SIN inhibitory phosphatase (SIP) complex related to the STRIPAK phosphatase complex is one inhibitor of SIN signaling. The SIP consists of Csc1, Csc2, Csc3, Csc4, Paa1, and the phosphatase subunit Ppa3. Here, we determine that the SIP is anchored at the SPB via the Csc1 FHA domain and that constitutive SPB localization of the SIP is lethal due to persistent SIN inhibition. Disrupting SIP docking at the SPB with a point mutation within the FHA domain or eliminating phosphatase activity by introducing a point mutation within Ppa3 resulted in intact SIP complexes without SIN inhibitory function. Lastly, we defined the unique features of Ppa3 that allow it, but not two other PP2A catalytic subunits, to incorporate into the SIP. Overall, we provide insight into how the SIP complex assembles, localizes, and functions to counteract the SIN with spatiotemporal precision during cytokinesis.**

Monitoring Editor
Rong Li
Johns Hopkins University and National University of Singapore

Received: Apr 29, 2024
Revised: May 29, 2024
Accepted: Jun 4, 2024

New Hypothesis

Cross-Validation

SIGNIFICANCE STATEMENT

- In *Schizosaccharomyces pombe*, the septation initiative network (SIN) ensures cytokinesis is coordinated with chromosome segregation. The PP2A SIN inhibitory phosphatase (SIP), analogous to human STRIPAK, inhibits the SIN but how it localizes is poorly understood.
- The authors report that the FHA domain in one SIP component is necessary and sufficient for SIP spindle pole body (SPB) targeting and function. Cell viability requires SPB SIP localization is transient. Residues unique to its catalytic subunit, Ppa3, specify its assembly into SIP.
- The findings highlight similarities and differences between SIP and STRIPAK and invite further study of the signaling pathway architectures controlling each.

This article was published online ahead of print in MBoC in Press (http://www.molbiolcell.org/cgi/doi/10.1091/mbc.E24-04-0196) on June 12, 2024.

*Address correspondence to: Kathleen L. Gould (kathy.gould@vanderbilt.edu).

Abbreviations used: AF, AlphaFold3; CR, cytokinetic ring; GBP, GFP binding protein; mNG, mNeonGreen; pLDDT, predicted local difference distance test ; PP2A, protein phosphatase 2A; SIN, septation initiation network; SIP, SIN inhibitory phosphatase; SPB, spindle pole body.

INTRODUCTION

In animals and fungi, cytokinesis is facilitated by an actin- and myosin-based cytokinetic ring (CR) (Pollard, 2010; Cheffings *et al.*, 2016; Glotzer, 2017; Mangione and Gould, 2019). In the yeast *Schizosaccharomyces pombe*, a GTPase-controlled signaling pathway named the septation initiation network (SIN), analogous to the Hippo pathway of multicellular eukaryotes, is essential for proper CR assembly, constriction, and the coordinate process of septation (reviewed in [Simanis, 2015; Cullati and Gould, 2019; Xiao and Dong, 2021]). Inactivation of SIN signaling results in elongated multinucleate inviable *S. pombe* cells due to repeated rounds of nuclear division and

cell growth in the absence of cell division. Reciprocally, constitutive SIN activity leads to the formation of multiple CRs and septa in the absence of nuclear division and is also lethal.

The SIN is assembled at spindle pole bodies (SPBs) by two SPB scaffold proteins, Sid4 and Cdc11, that are responsible for recruiting all downstream components of the pathway (Morrell *et al.*, 2004). SIN signaling is initiated with spindle formation at metaphase when the GTPase, Spg1, is activated at both separated SPBs and its effector protein kinase Cdc7 begins to accumulate at both SPBs (Schmidt *et al.*, 1997; Sohrmann *et al.*, 1998; Wachowicz *et al.*, 2015). As anaphase progresses, Spg1-Cdc7 localization symmetry is broken with Cdc7 loss at the old SPB (Schmidt *et al.*, 1997; Grallert *et al.*, 2004) and Cdc7 increasing in abundance at the new SPB that retains active Spg1 (Sohrmann *et al.*, 1998; Garcia-Cortes and McCollum, 2009). The Sid1 protein kinase complex then localizes with active Spg1-Cdc7 at the new SPB (Guertin *et al.*, 2000). The persistence of symmetrical localization of Cdc7 during anaphase, or precocious localization of Cdc7 to SPBs during interphase, correlates with elevated SIN activity (Sohrmann *et al.*, 1998). The final SIN protein kinase, Sid2, also localizes to SPBs but independently of Spg1 (Sparks *et al.*, 1999). Unlike the aforementioned SIN components, the Sid2-Mob1 protein kinase complex localizes to the CR when Sid1 binds the SPB (Sparks *et al.*, 1999; Hou *et al.*, 2000; Salimova *et al.*, 2000). Sid2 activity is necessary for the establishment of SIN asymmetry at SPBs (Feoktistova *et al.*, 2012) and Sid2-mediated phosphorylation events at the CR are considered to provide the final output of the SIN (reviewed in [Bohnert and Gould, 2011; Johnson *et al.*, 2012]).

The essential proteins Byr4 and Cdc16 comprise the Spg1 GAP, and in the *cdc16-116* mutant at restrictive temperature, cells septate uncontrollably regardless of cell cycle stage and die (Minet *et al.*, 1979; Furge *et al.*, 1998). These major SIN inhibitors localize in a reciprocal manner to Cdc7; they are at the SPB during interphase preventing Spg1 activation, transiently leave the SPBs during early mitosis when Cdc7 localizes to both SPBs, and then localize to the old SPB during anaphase (Li *et al.*, 2000).

SIN inhibitory phosphatase (SIP) is another SIN inhibitor (Singh *et al.*, 2011). SIP is a nonessential multiprotein phosphatase 2A (PP2A) complex analogous to STRIPAK in multicellular eukaryotes (Kuck *et al.*, 2019) that is a negative inhibitor of the SIN-related Hippo pathway (Ribeiro *et al.*, 2010). The SIP is comprised of a specific PP2A catalytic subunit named Ppa3, a scaffold component shared with other PP2A complexes termed Paa1, and four proteins unique to the SIP complex: Csc1/Far10/SLMAP, Csc2/Far11/STRIP, Csc3/Far8/striatin, and Csc4/SIKE (Singh *et al.*, 2011). Loss of SIP-specific components results in symmetrical Cdc7 and Sid1 localization to both SPBs during anaphase, loss of Byr4 from both SPBs, and a mild gain-of-function SIN phenotype (Singh *et al.*, 2011). As expected of a second SIN inhibitor, null mutants of SIP components display negative genetic interactions with the *cdc16-116* mutant (Singh *et al.*, 2011).

Like other SIN components and regulators, the SIP complex shows a dynamic SPB localization pattern. SIP components localize to both SPBs during metaphase and then only the opposite SPB to that of Cdc7 and Sid1 during anaphase; they do not localize to SPBs during interphase and mitotic Cdk1 activity is required to recruit the SIP to SPBs during mitosis (Singh *et al.*, 2011). There, mitotically phosphorylated Cdc11 is thought to be a significant SIP substrate at the SPB (Singh *et al.*, 2011). However, neither Cdc11 nor any other SIN component is required for SIP localization to SPBs (Singh *et al.*, 2011), and therefore how precisely the SIP is recruited to the SPB is unclear. It is also not known whether SPB localization is required for SIP function in cytokinesis.

Here we determined that the FHA domain of Csc1/Far10/SLMAP is necessary and sufficient for localizing SIP to the mitotic SPBs. A mutation that disrupts SIP–SPB interaction does not affect SIP complex formation but abrogates SIP function in SIN inhibition. Tethering the SIP to the SPB results in lethality due to chronic SIN inhibition and this can partially rescue Cdc16 loss-of-function. We also demonstrate that SIN inhibition by SIP requires the function of the SIP-specific catalytic subunit, Ppa3, and that phosphatase activity is not required for SIP SPB localization.

RESULTS AND DISCUSSION

Identification of the FHA domain as a SPB localization cue

The ability of Csc1, Csc2, and Csc3 to localize to the SPB depends on all other components of the complex being present (Singh *et al.*, 2011). We found that this is also true for Csc4. Csc4-GFP was not detected at SPBs in *csc1Δ, csc2Δ, csc3Δ* or *ppa3Δ* cells (Supplemental Figure S1A). This suggests that the SIP complex must be intact to localize correctly, and that loss of any single component disrupts the complex. Thus, it is unclear which component(s) directs SIP–SPB localization. The SLMAP component of STRIPAK, through its forkhead-associated (FHA) domain, is necessary to bind MST2 for inhibition of the Hippo pathway (Couzens *et al.*, 2013; Bae *et al.*, 2017; Zheng *et al.*, 2017; Tang *et al.*, 2019). Csc1 contains the orthologous FHA domain (Figure 1A) and we therefore tested whether it was necessary to direct SIP to SPBs.

A mutation was introduced into the endogenous *csc1* locus that resulted in a R31A substitution within the FHA domain (Figure 1A). By analogy with SLMAP and other FHA domains, this mutation is predicted to disrupt FHA domain interaction with phosphorylated residues (Durocher and Jackson, 2002; Bae *et al.*, 2017; Zheng *et al.*, 2017). We first examined whether the SIP complex remained intact with the Csc1-R31A substitution. The Csc1-R31A mutant was tagged with GFP and combined with TAP-tagged versions of the SIP components Csc2-TAP, Csc3-TAP, and Csc4-TAP. The SIP phosphatase catalytic subunit, Ppa3, cannot be tagged without loss of function (Singh *et al.*, 2011). In all three tested strains, pull-downs with an antibody to GFP led to the coimmunoprecipitation of the other tagged subunits (Figure 1B). These results indicate that the *csc1-R31A* mutation does not disrupt SIP complex formation.

We next examined the localization of Csc1-R31A-GFP. Using Sid4-RFP as a marker of SPBs (Chang and Gould, 2000), we did not detect Csc1-R31A-GFP on SPBs at any point in the cell cycle (Figure 1C). We also did not detect Csc2-GFP, Csc3-GFP or Csc4-GFP at SPBs in *csc1-R31A* cells although these proteins were detected at SPBs in wildtype cells (Supplemental Figure S1B). We conclude that the FHA domain is required for targeting SIP to SPBs.

We next asked whether the Csc1 FHA domain was sufficient for SPB targeting. We exogenously expressed GFP-Csc1(FHA) from the *nmt81* promoter of pREP81 in cells producing Sad1-mCherry as a SPB marker (Hagan and Yanagida, 1995) and found that GFP-Csc1(FHA) localized to SPBs in mitotic cells (Figure 1D). However, GFP-Csc1(FHA-R31A) was not detected at any SPBs (Figure 1D). Similarly, the FHA domain of SLMAP is required for directing the STRIPAK phosphatase complex to its substrate in the Hippo pathway, Hpo/MST (Couzens *et al.*, 2013; Bae *et al.*, 2017; Zheng *et al.*, 2017). In conclusion, the Csc1 FHA domain is necessary and sufficient to direct the SIP to SPBs during mitosis.

Lastly, as expected, we also found that the SPB localization of GFP-Csc1(FHA), like that of Csc1-GFP (Singh *et al.*, 2011), is independent of the SIN because GFP-Csc1(FHA) expressed from the

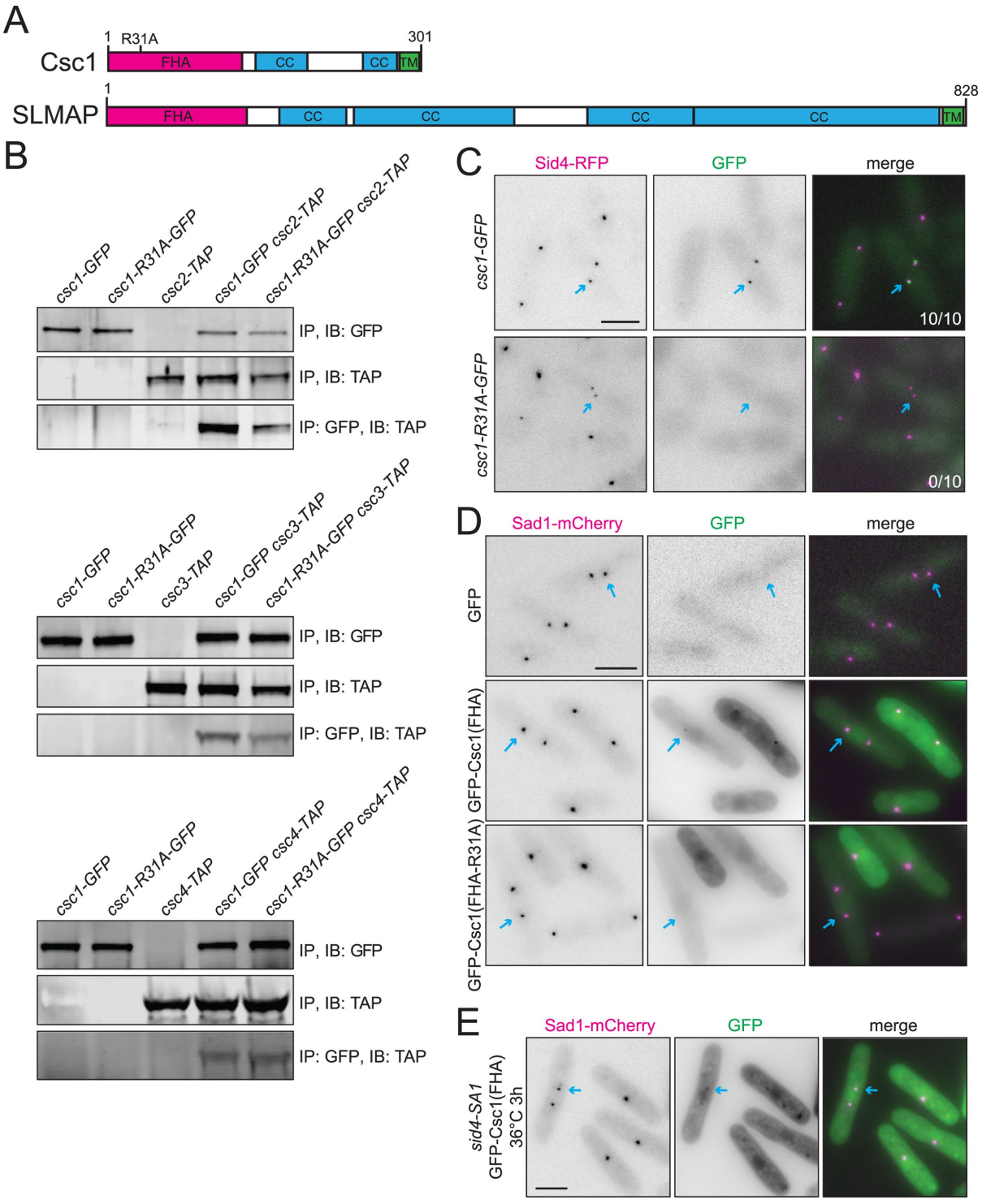

FIGURE 1: The SIP complex remains intact without a functional FHA domain. (A) A schematic of Csc1 compared with human SLMAP, drawn to scale, with predicted coiled-coil (CC) and transmembrane (TM) domains and the position of R31A mutation indicated. (B) Anti-GFP immunoprecipitation and immunoblot (top panel), anti-IgG immunoprecipitation and immunoblot (middle panel) or anti-GFP immunoprecipitation with anti-IgG immunoblot (bottom panel) from the indicated strains. (C) Live-cell imaging of cells expressing Csc1-GFP or Csc1-R31A-GFP with Sid4-RFP. The numbers in the bottom right corner of the merged images indicate the number of early mitotic cells with Csc1 SPB localization over the total number of early mitotic cells counted. Blue arrows indicate a cell in anaphase. (D) Live-cell imaging of *sad1-mCherry* cells induced to express *GFP*, *GFP-Csc1(FHA)* or *GFP-Csc1(FHA-R31A)* from the *nmt81* promoter for 18 h before imaging at 25°C. (E) Live-cell imaging of *sid4-SA1 sad1-mCherry* cells induced to express *GFP-Csc1(FHA)* for 24 h. The cells were grown up at 25°C and then shifted to 36°C for 3 h before imaging. (C, D, and E) Blue arrows indicate an early mitotic SPB. Scale bars, 5 μm.

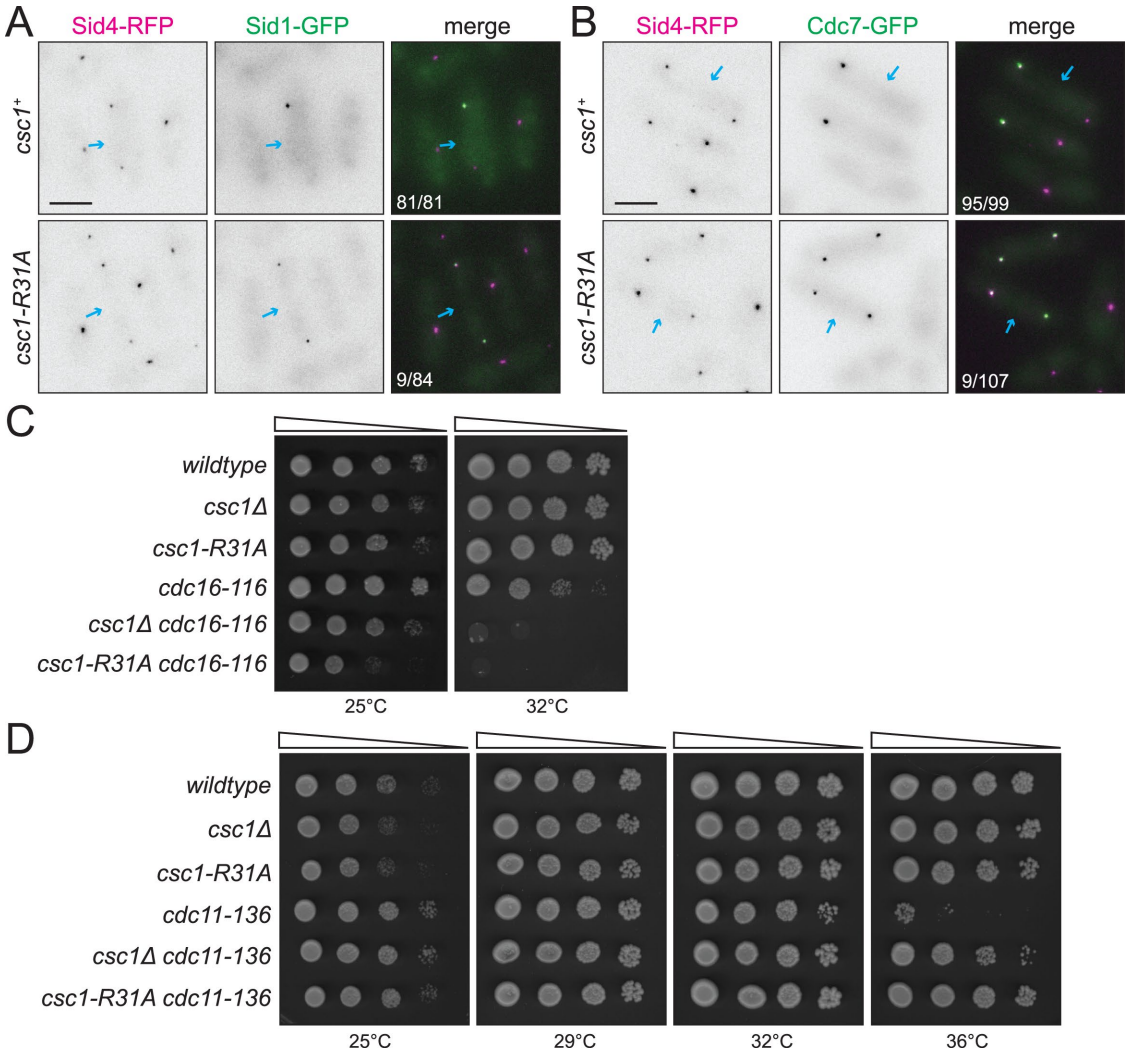

FIGURE 2: SIP localization to the SPB and SIN inhibition depends on the Csc1 FHA domain. (A and B) Live-cell imaging of wildtype and *csc1-R31A* cells expressing Sid1-GFP (A) or Cdc7-GFP (B) with Sid4-RFP. The numbers in the bottom right corner of the merge images indicates the number of cells with asymmetric SPB localization in late anaphase over the total number of cells counted. Blue arrows indicate a cell in anphase. (C and D) 10-fold serial dilutions of the indicated strains grown at the indicated temperatures for 3–4 d on YE agar. Scale bars, 5 μm.

nmt81 promoter of pREP81 localized to mitotic SPBs marked by Sad1-mCherry in the SIN scaffold mutant *sid4-SA1* cells at the restrictive temperature (Figure 1E).

SIP SPB localization is required for its function

Based on its role as a SIN inhibitor, we predicted that SPB localization would be essential for SIP function. As a measure of SIP function, we examined the localization of Cdc7 and Sid1 in mitotic *csc1-R31A* cells. As in SIP deletion mutants (Singh *et al.*, 2011), we found that Cdc7 and Sid1 localized symmetrically to both SPBs during anaphase in contrast to its asymmetrical distribution to a single SPB in wildtype anaphase cells (Figure 2, A and B).

Null mutants in the SIP display a negative genetic interaction with a mutation in *cdc16* (Singh *et al.*, 2011). Thus, we tested whether *csc1-R31A* interacted negatively with *cdc16-116* cells and found that it did (Figure 2C). SIP null mutants rescue *cdc11-136* (Singh *et al.*, 2011) and we observed that *csc1-R31A* also did (Figure 2D). We conclude that the ability of SIP to localize to SPBs during mitosis is necessary for its function as a SIN inhibitor.

Constitutive SIP SPB localization is lethal

The SIP is detected on SPBs only during mitosis (Singh *et al.*, 2011). To determine whether the SIP needs to be released from SPBs at other cell cycle stages, we used the GFP–GFP binding protein (GBP) system to artificially tether Csc1-GFP to the SPB by combining it with Sid4-GBP-mCherry or Ppc89-GBP-mCherry (Rothbauer *et al.*, 2006, 2008). Ppc89 is a core SPB protein that tethers the SIN through a direct interaction with Sid4 (Rosenberg *et al.*, 2006). Interestingly, we found that cells producing both Csc1-GFP and either Ppc89-GBP-mCherry (Supplemental Figure S2A) or Sid4-GBP-mCherry (Figure 3A) were inviable. This result indicates that dynamic SIP SPB localization is critical. We found that cells producing both Csc1-R31A-GFP and Ppc89-GBP-mCherry (Supplemental Figure S2B) or Sid4-GBP-mCherry (Figure 3B) were also inviable. Microscopic observation of the inviable cells showed they died as single elongated cells, consistent with SIN inactivation (Supplemental Figure S2, C and D). To confirm that the cells died due to SIN failure, we expressed *csc1-GBP-mCherry* from the regulatable *nmt81* promoter in either wildtype or *ppc89-GFP* cells. In wildtype cells,

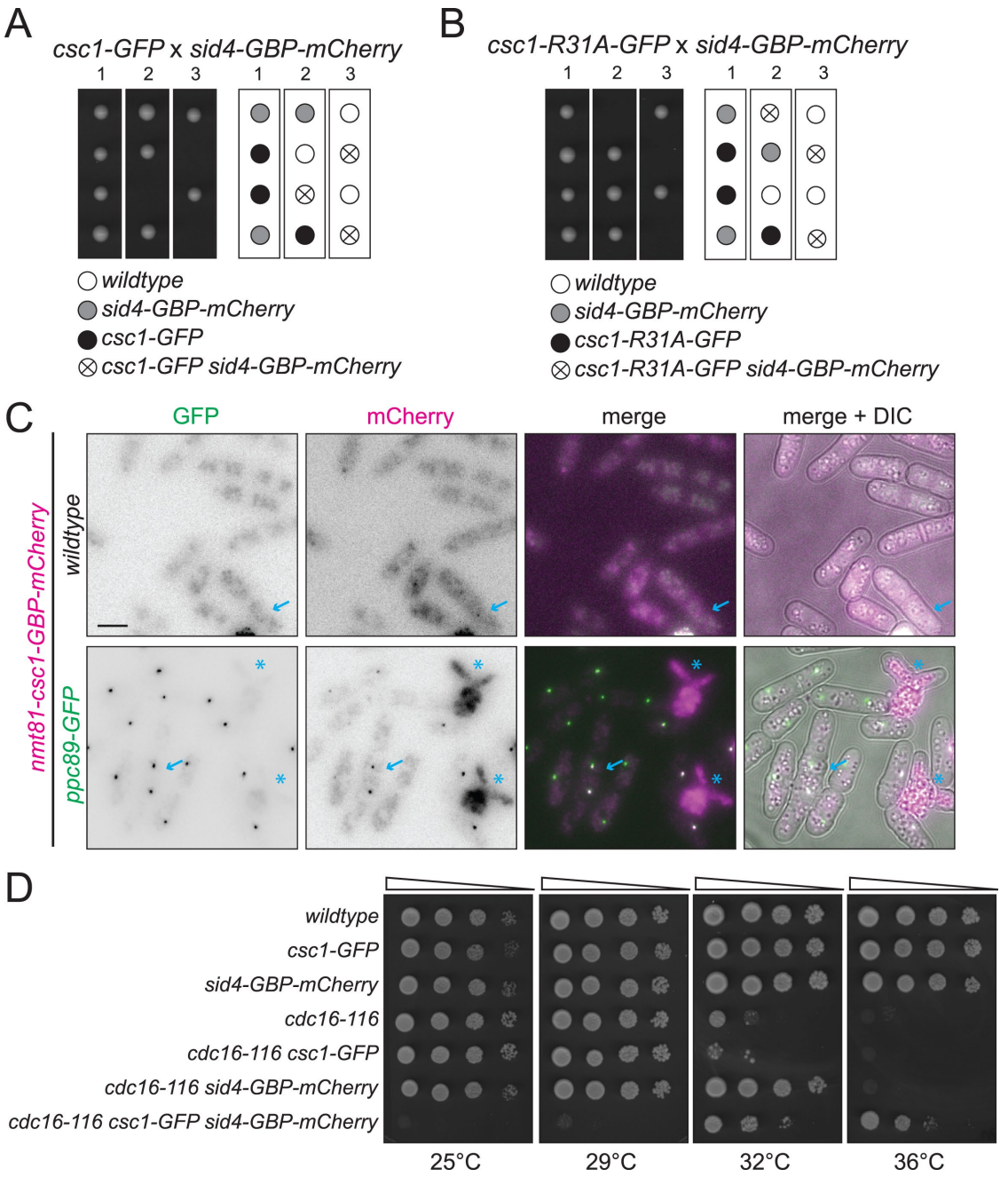

FIGURE 3: Artificially tethered Csc1 to the SPB is lethal. (A and B) Representative tetrads and schematic of tetrad analysis from the indicated genetic cross. (C) Live-cell imaging of wildtype or *ppc89-GFP* cells with *nmt81-csc1-GBP-mCherry* expression induced for 30 h before imaging. Blue arrows indicate an example cell with Csc1-GBP-mCherry localized to a SPB. Blue asterisks indicate lysed cells. Scale bar, 5 µm. (D) 10-fold serial dilutions of the indicated strains grown at the indicated temperatures for 3 d on YE agar.

Csc1-GBP-mCherry localized to early mitotic SPBs but otherwise was diffuse in the cytoplasm and no cell defects were observed (Figure 3C). In contrast, Csc1-GBP-mCherry localized to most SPBs in *ppc89-GFP* cells and many of these cells failed cytokinesis or lysed at division, both phenotypes typical of defects in SIN function (Figure 3C). These results indicate that the SIP complex containing Csc1-R31A retains SIN-inhibitory function so long as it localizes to the SPB and that tethering the SIP complex to the SPB causes lethality due to constitutive SIN inhibition.

We next tested whether cells with overactive SIN signaling (e.g., defective in Cdc16 function) might tolerate chronic SIP-SPB anchoring. To test this possibility, we constructed *cdc16-116 csc1-GFP* and *cdc16-116 sid4-GBP-mCherry* strains and crossed them to generate a *cdc16-116 csc1-GFP sid4-GBP-mCherry* strain. We were able to recover the *cdc16-116 csc1-GFP sid4-GBP-mCherry* strain when, after tetrad dissection, spores were placed at the semipermissive temperature for *cdc16-116* of 32°C (Supplemental Figure S2, E and F). By antagonizing *cdc16-116* gain of function, cells with SIP tethered to the SPB grew at 32°C and even 36°C (Figure 3D). However, these cells died at 25°C when the SIN would be chronically inhibited by SIP (Figure 3D).

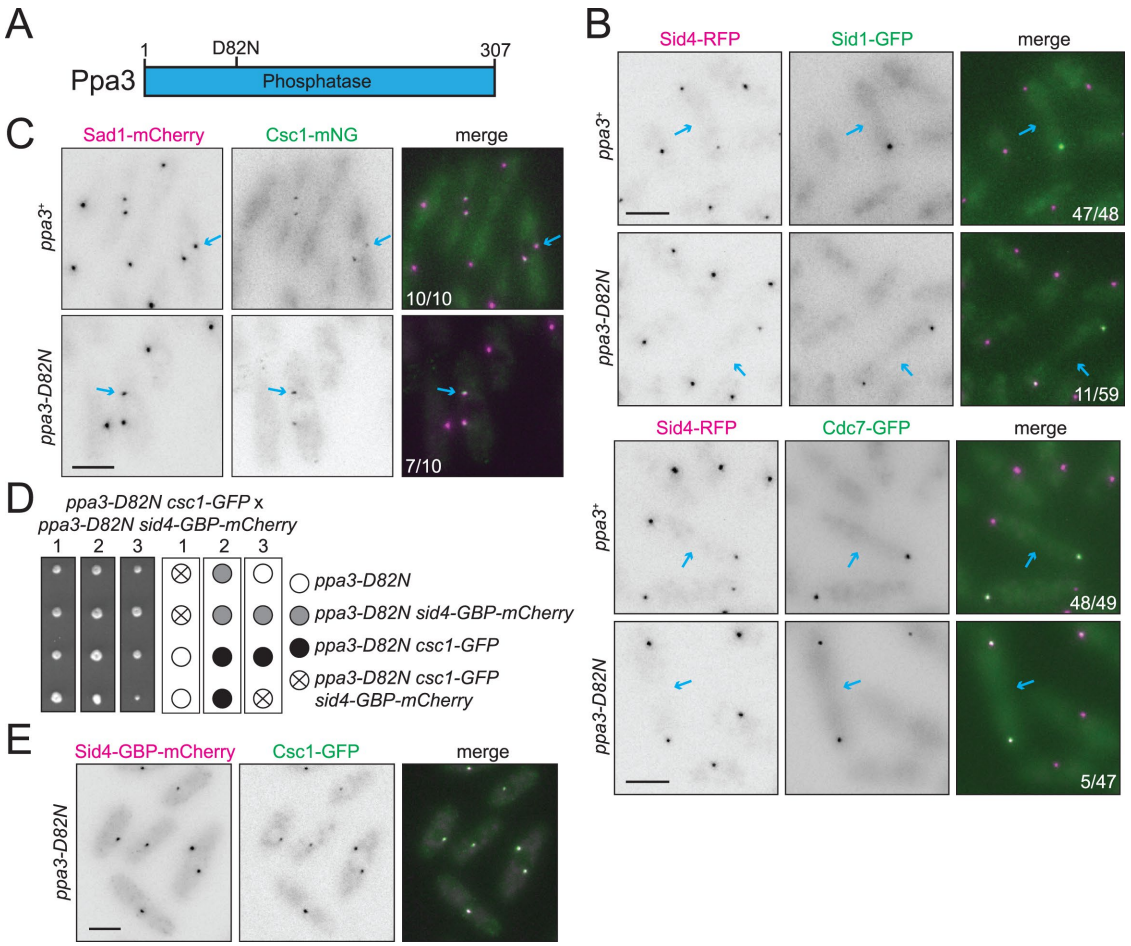

FIGURE 4: Ppa3 phosphatase activity is required for SIP function. (A) A schematic of Ppa3, drawn to scale, with the position of the D82N mutation indicated. (B) Live-cell imaging of wildtype and *ppa3-D82N* expressing either Sid1-GFP or Cdc7-GFP with Sid4-RFP. The numbers in the bottom right corner of the merge images indicates the number of cells with asymmetric SPB localization in late anaphase over the total number of cells counted. Blue arrows indicate a cell in anaphase. (C) Live-cell imaging of Csc1-mNG Sad1-mCherry in wildtype or *ppa3-D82N* cells. Blue arrows indicate an early mitotic SPB. The numbers in the bottom left corner of the merged images indicate the number of early mitotic cells with Csc1 SPB localization over the total number of early mitotic cells counted. (D) Representative tetrads and schematic of tetrad analysis from the indicated genetic cross. (E) Live-cell imaging of *ppa3-D82N csc1-GFP sid4-GBP-mCherry* cells grown at 25°C before imaging. Scale bars, 5 μm.

The activity of the Ppa3 catalytic subunit is required for SIP function

To validate that SIP-dependent SIN inhibition is dependent on SIP phosphatase activity, we replaced endogenous *ppa3* with a mutation that, based on homology with other catalytic subunits, is predicted to eliminate Ppa3 phosphatase activity (Zhuo *et al.*, 1994; Myles *et al.*, 2001; Figure 4A). Like *ppa3*Δ, *ppa3-D82N* cells were viable and rescued growth of *cdc11-136*, an indication that it is a loss-of-function *ppa3* allele (Supplemental Figure S3A). As another readout for SIP function, we analyzed Sid1 and Cdc7 localization in wildtype and *ppa3-D82N* cells. *ppa3-D82N* cells producing Sid4-RFP displayed symmetric Sid1-GFP and Cdc7-GFP localization on anaphase SPBs whereas the localization is asymmetric in wildtype cells (Figure 4B). This further demonstrates that *ppa3-D82N* is a loss of function allele.

Because some PP2A catalytic subunit site mutants disrupt binding to other PP2A subunits (Ogris *et al.*, 1999; Lizotte *et al.*, 2008), we analyzed SIP component localization to confirm that the complex remains intact in *ppa3-D82N* cells. In both wildtype and *ppa3-D82N* cells, Csc1-GFP localized to mitotic SPBs (Figure 4C). Thus, the ability of the SIP complex to assemble and localize properly is independent of its phosphatase activity.

Lastly, we predicted that constitutive tethering of the SIP to SPBs would be tolerated if Ppa3 lacked catalytic activity. To test this, we constructed *ppa3-D82N csc1-GFP* and *ppa3-D82N sid4-GBP-mCherry* strains, crossed them, and found that the *ppa3-D82N csc1-GFP sid4-GBP-mCherry* strain could be recovered (Figure 4D). Live-cell imaging of *ppa3-D82N csc1-GFP sid4-GBP-mCherry* cells confirmed that in this strain Csc1-GFP was constitutively tethered to the SPB (Figure 4E). In conclusion, both dynamic SPB localization and Ppa3-specific phosphatase activity are required for proper SIP function.

Identification of SIP-specific features of Ppa3

While all three *S. pombe* PP2A catalytic subunits bind Paa1, the PP2A A subunit (Singh *et al.*, 2011; Bernal *et al.*, 2014), neither Ppa1 nor Ppa2 are assembled into the SIP complex (Singh *et al.*, 2011). We thus predicted that Ppa3 contains unique sequences relative to Ppa1 and Ppa2 that allow it to integrate into the SIP despite Ppa1 and Ppa2 being ~55% identical and ~67% similar to Ppa3

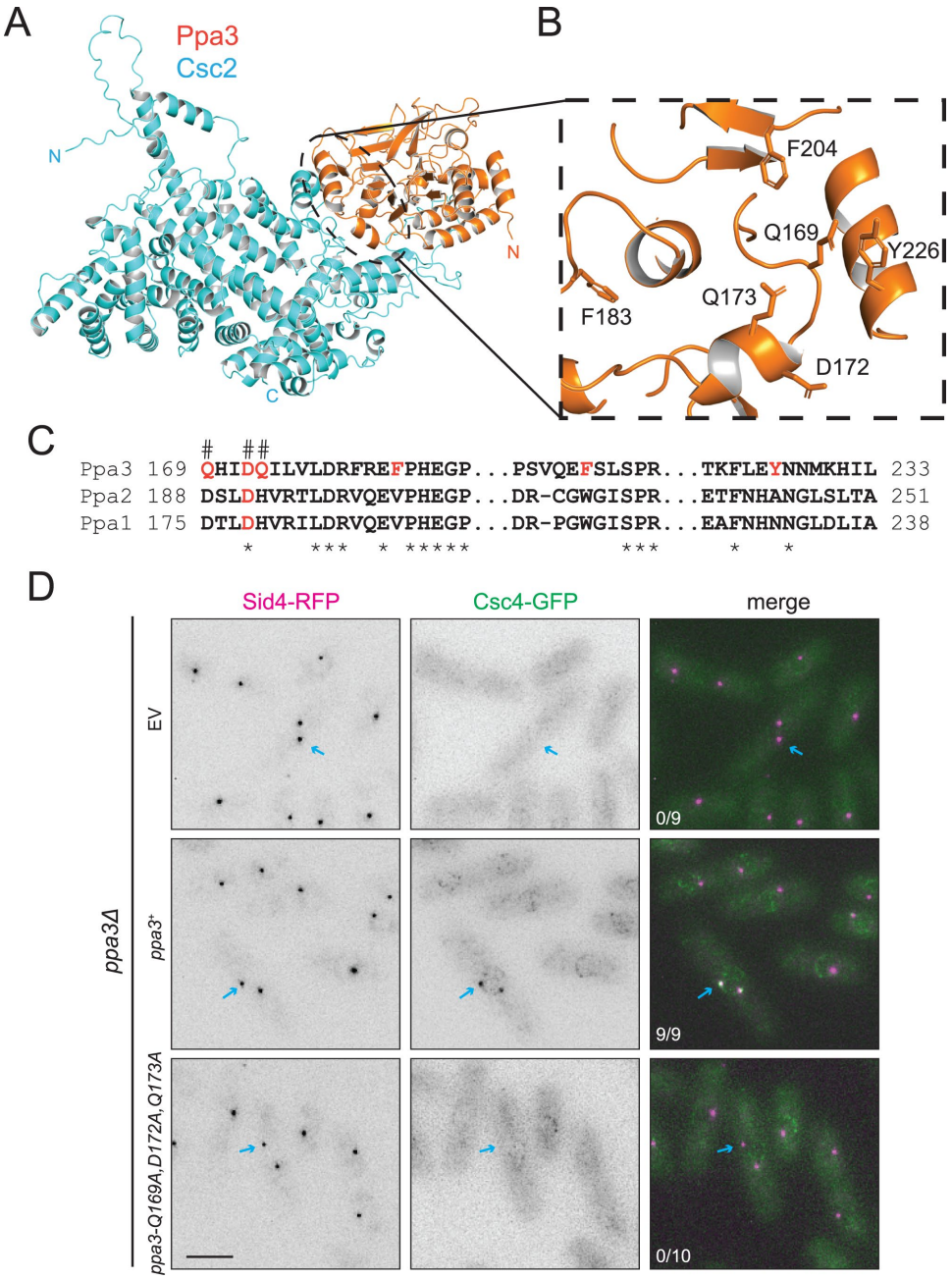

FIGURE 5: Ppa3 contains unique features that direct it to the SIP complex. (A) AF generated prediction of the Ppa3-Csc2 complex. Full-length sequences of each protein were analyzed. Ppa3 is in orange and Csc2 is in blue. (B) A zoomed in view of the predicted Ppa3 interaction surface. Residues that are predicted to mediate the Csc2 interaction are labeled. (C) A sequence alignment of the indicated *S. pombe* proteins. Ppa3 residues necessary for binding Csc2 are highlighted in orange and conserved residues are indicated with an asterisk. Q169, D172, and Q173 are indicated with a "#." (D) Live-cell imaging of *ppa3Δ csc4-GFP sid4-RFP* cells expressing the indicated constructs. Blue arrows indicate an early mitotic SPB. The numbers in the bottom left corner of the merged images indicate the number of early mitotic cells with Csc4 SPB localization over the total number of early mitotic cells counted. Scale bar, 5 μm.

(Supplemental Figure S3B). A crystal structure of the human STRIPAK complex revealed that the PP2A catalytic subunit directly binds the STRIP1 subunit (Jeong *et al.*, 2021). In *S. pombe*, the STRIP1 analogue is Csc2, and we thus interrogated the Ppa3-Csc2 interaction using AlphaFold3 (AF; Abramson *et al.*, 2024). AF predicted a Ppa3-Csc2 interaction with high confidence (predicted Local Difference Distance Test [pLDDT] = ~90–95) and the predicted interface was similar to that in the human STRIPAK structure (Figure 5, A and B; Jeong *et al.*, 2021). Interestingly, five of the six Ppa3 residues predicted to directly bind Csc2 are unique to Ppa3 relative to Ppa1 and Ppa2 (Figure 5, B and C; Supplemental Figure S3B). To test the AF model, we produced wildtype Ppa3 or Ppa3 variants with mutations in the predicted Csc2 interaction interface in *ppa3Δ csc4-GFP sid4-RFP* cells. As expected if the SIP complex was restored, Csc4-GFP was present at mitotic SPBs in cells expressing wildtype *ppa3*$^{+}$, but not an empty vector control (Figure 5D). In contrast, Csc4-GFP was not localized to SPBs in cells expressing *ppa3-Q169A,D172A,Q173A* (Figure 5D) but it was detected at SPBs in *ppa3-F183A* or *ppa3-Y226A* expressing cells (Supplemental Figure S3C). These results indicate that Q169, D172, and Q173 are important for linking Ppa3 into the SIP complex while F183 and Y226 are not. Other residues unique to Ppa3 may also be involved.

In sum, our work has demonstrated further similarities between SIP and STRIPAK complexes and also highlighted their differences. First, although PP2A catalytic subunits are components of both phosphatase complexes, SIP has a dedicated catalytic subunit, Ppa3, the activity of which we have shown is required for SIN inhibition. Further, we have defined sequences in one of three highly conserved *S. pombe* PP2A catalytic subunits necessary for its selective incorporation into the SIP. Why *S. pombe* evolved a specific catalytic subunit for the SIP complex is not clear but it may allow the SIP inhibition of the SIN to be controlled solely by the activity of a cell cycle kinase(s). Second, while the FHA domains of both Csc1 and SLMAP are required for the proper localization of the phosphatase complexes, the cue for Csc1-FHA domain localization and the target of SIP activity (e.g., the SIN) are distinct. This signaling architecture differs from that in fly and mammalian cells in which STRIPAK binds its Hippo substrate directly via the FHA domain of SLMAP (Couzens *et al.*, 2013; Bae *et al.*, 2017; Zheng *et al.*, 2017). To understand the signaling logic more precisely, future studies can be aimed at identifying the molecular cue for Csc1 FHA domain SPB localization in mitotic cells.

MATERIALS AND METHODS

Request a protocol through *Bio-protocol*.

Strains and media

S. pombe strains (Supplemental Table S1) were grown in yeast extract or minimal medium with appropriate supplements (Moreno *et al.*, 1991). Transformations were performed by the lithium acetate method (Keeney and Boeke, 1994; Gietz *et al.*, 1995). Epitope-tagged strains were constructed as described previously (Wach *et al.*, 1994; Bahler *et al.*, 1998) so that open reading frames were tagged at the 3′ end of endogenous loci with the *GFP:kanMX6*, *mNG:kanMX6*, *mNG:hphMX6*, or *TAP:kanMX6* cassettes. Appropriate tagging was confirmed by whole-cell PCR, live-cell imaging, and/or immunoblotting. Strain construction and tetrad analysis were accomplished through standard methods.

The *csc1-R31A* strain was made by cloning the open reading frame of *csc1*$^{+}$ with 500 bp of the 5′ and the 3′ flanking sequences cloned into the PstI/BamHI sites of pIRT2. The R31A mutation was made by site directed mutagenesis and confirmed with sequencing. The pIRT2-*csc1-R31A* was transformed into a haploid *csc1Δ::ura4*$^{+}$ strain and colonies were selected on YE plates containing 1.5 mg/ml 5-fluoroorotic acid and validated by whole-cell PCR and DNA sequencing.

pREP81GFP-*csc1(FHA)* was constricted by amplifying residues 1-390 of *csc1* from genomic DNA and cloning into NdeI/BamHI sites of pREP81GFP via Gibson assembly. The R31A mutation was introduced using site-directed mutagenesis and confirmed by DNA sequencing. The vectors were transformed into *sad1-mCherry* cells using a sorbitol transformation protocol (Moreno *et al.*, 1991). The cells were grown at 25°C in minimal media containing adenine, uracil and 5 μM thiamine and then washed into media lacking thiamine for 24 h before imaging. For visualization in *sid4-SA1* cells, cells were shifted to 36°C for 3 h before imaging.

The *ppa3-D82N* strain was made by cloning the open reading frame of *ppa3*$^{+}$ with 500 bp of the 5′ and 3′ flanking sequences cloned into the XmaI/PstI sites of pIRT2. The D82N mutation was made by site directed mutagenesis and confirmed with sequencing. the pIRT2-*ppa3-D82N* was transformed into *ppa3Δ::ura4*$^{+}$ strain and colonies were selected on YE plates containing 1.5 mg/ml 5-fluoroorotic acid and validated by whole-cell PCR and DNA sequencing.

pREP1-*ppa3*$^{+}$ was constructed by amplifying the coding sequence from genomic DNA and performing Gibson cloning to insert the sequence at the NdeI/BamH1 sites. The cloning was confirmed by sequencing.

Immunoprecipitations and immunoblotting

Whole-cell lysates were prepared in NP-40 buffer (6 mM Na_2HPO_4, 4 mM NaH_2PO_4, 1% NP-40, 150 mM NaCl, 50 mM NaF, 0.1 mM Na_3VO_4, 2 mM EDTA, 1 mM phenylmethylsulfonyl fluoride, 2 mM benzamidine, 0.5 mM diisopropyl fluorophosphate, 5 μg/ml leupeptin) and protease inhibitor tablet (cOmplete Protease Inhibitor Cocktail, Roche) in native conditions as previously described (Gould *et al.*, 1991). Proteins were immunoprecipitated from protein lysates using anti-GFP (Vanderbilt Antibody and Protein Resource Core, VUIC9A5) followed by Protein G Sepharose beads (Cytiva) or a polyclonal anti-IgG (Vanderbilt Antibody and Protein Resource Core) followed by Protein A Sepharose beads (Cytiva).

For immunoblotting, proteins were resolved by 3–8% Tris-acetate PAGE or 4–12% NuPAGE, transferred by electroblotting to a polyvinylidene difluoride membrane (Immobilon FL; Millipore Sigma) and incubated with the set of primary antibodies indicated at 1 μg/ml. Primary antibodies were detected with secondary antibodies coupled to IRDye680 or IRDye800 (LI-COR Biosciences) and visualized using an Odyssey Imaging System (LI-COR Biosciences).

Microscopy

Yeast cells were grown at 25°C in YE before live-cell imaging and acquired with a Zeiss Axio Observer inverted epifluorescence microscope with Zeiss 63X oil (1.46 NA) and captured using Zeiss ZEN 3.0 (Blue edition) software and Axiocam 503 monochrome camera (Zeiss). Images in figures are nondeconvolved maximum intensity projections.

Protein structure prediction and sequence alignment

Protein structure predictions were generated with the AF3 server (Abramson *et al.*, 2024). Protein sequence alignments were performed using Clustal Omega (Sievers and Higgins, 2021; Madeira *et al.*, 2022).

DATA AVAILABILITY STATEMENT

The data underlying Figures 1–5 and Supplemental Figures 1–3 are openly available in Mendeley Data at doi: 10.17632/r4nww6c58k.1 and 10.17632/nf8wsrc79d.1.

ACKNOWLEDGMENTS

We thank Drs. Kazutoshi Akimura and Jun-Song Chen for critical reading of the manuscript. We also thank Dr. Brian Wadzinski and Dr. Mark Swingle for recommending the Ppa3-D82N mutation. This work was supported by National Insitutes of Health grant R35GM131799 to K.L.G.

REFERENCES

Abramson J, Adler J, Dunger J, Evans R, Green T, Pritzel A, Ronneberger O, Willmore L, Ballard AJ, Bambrick J, *et al.* (2024). Accurate structure prediction of biomolecular interactions with AlphaFold 3. Nature 630, 493–500.

Bae SJ, Ni L, Osinski A, Tomchick DR, Brautigam CA, Luo X (2017). SAV1 promotes Hippo kinase activation through antagonizing the PP2A phosphatase STRIPAK. eLife 6, e30278.

Bahler J, Wu JQ, Longtine MS, Shah NG, McKenzie A, 3rd, Steever AB, Wach A, Philippsen P, Pringle JR (1998). Heterologous modules for efficient and versatile PCR-based gene targeting in *Schizosaccharomyces pombe*. Yeast 14, 943–951.

Bernal M, Zhurinsky J, Iglesias-Romero AB, Sanchez-Romero MA, Flor-Parra I, Tomas-Gallardo L, Perez-Pulido AJ, Jimenez J, Daga RR (2014). Proteome-wide search for PP2A substrates in fission yeast. Proteomics 14, 1367–1380.

Bohnert KA, Gould KL (2011). On the cutting edge: post-translational modifications in cytokinesis. Trends Cell Biol 21, 283–292.

Chang L, Gould KL (2000). Sid4p is required to localize components of the septation initiation pathway to the spindle pole body in fission yeast. Proc Natl Acad Sci USA 97, 5249–5254.

Cheffings TH, Burroughs NJ, Balasubramanian MK (2016). Actomyosin Ring Formation and Tension Generation in Eukaryotic Cytokinesis. Curr Biol 26, R719–R737.

Couzens AL, Knight JD, Kean MJ, Teo G, Weiss A, Dunham WH, Lin ZY, Bagshaw RD, Sicheri F, Pawson T, *et al.* (2013). Protein interaction network of the mammalian Hippo pathway reveals mechanisms of kinase-phosphatase interactions. Sci Signal 6, rs15.

Cullati SN, Gould KL (2019). Spatiotemporal regulation of the Dma1-mediated mitotic checkpoint coordinates mitosis with cytokinesis. Curr Genet 65, 663–668.

Durocher D, Jackson SP (2002). The FHA domain. FEBS Lett 513, 58–66.

Feoktistova A, Morrell-Falvey J, Chen JS, Singh NS, Balasubramanian MK, Gould KL (2012). The fission yeast septation initiation network (SIN) kinase, Sid2, is required for SIN asymmetry and regulates the SIN scaffold. Mol Biol Cell 23, 1636–1645.

Furge KA, Wong K, Armstrong J, Balasubramanian M, Albright CF (1998). Byr4 and Cdc16 form a two-component GTPase-activating protein for the Spg1 GTPase that controls septation in fission yeast. Curr Biol 8, 947–954.

Garcia-Cortes JC, McCollum D (2009). Proper timing of cytokinesis is regulated by Schizosaccharomyces pombe Etd1. J Cell Biol 186, 739–753.

Gietz RD, Schiestl RH, Willems AR, Woods RA (1995). Studies on the transformation of intact yeast cells by the LiAc/SS- DNA/PEG procedure. Yeast 11, 355–360.

Glotzer M (2017). Cytokinesis in Metazoa and Fungi. Cold Spring Harb Perspect Biol 9, a022343.
Gould KL, Moreno S, Owen DJ, Sazer S, Nurse P (1991). Phosphorylation at Thr167 is required for *Schizosaccharomyces pombe* p34cdc2 function. EMBO J 10, 3297–3309.
Grallert A, Krapp A, Bagley S, Simanis V, Hagan IM (2004). Recruitment of NIMA kinase shows that maturation of the S. pombe spindle-pole body occurs over consecutive cell cycles and reveals a role for NIMA in modulating SIN activity. Genes Dev 18, 1007–1021.
Guertin DA, Chang L, Irshad F, Gould KL, McCollum D (2000). The role of the sid1p kinase and cdc14p in regulating the onset of cytokinesis in fission yeast. EMBO J 19, 1803–1815.
Hagan I, Yanagida M (1995). The product of the spindle formation gene sad1+ associates with the fission yeast spindle pole body and is essential for viability. J Cell Biol 129, 1033–1047.
Hou MC, Salek J, McCollum D (2000). Mob1p interacts with the Sid2p kinase and is required for cytokinesis in fission yeast. Curr Biol 10, 619–622.
Jeong BC, Bae SJ, Ni L, Zhang X, Bai XC, Luo X (2021). Cryo-EM structure of the Hippo signaling integrator human STRIPAK. Nat Struct Mol Biol 28, 290–299.
Johnson AE, McCollum D, Gould KL (2012). Polar opposites: Fine-tuning cytokinesis through SIN asymmetry. Cytoskeleton (Hoboken) 69, 686–699.
Keeney JB, Boeke JD (1994). Efficient targeted integration at leu1-32 and ura4-294 in *Schizosaccharomyces pombe*. Genetics 136, 849–856.
Kuck U, Radchenko D, Teichert I (2019). STRIPAK, a highly conserved signaling complex, controls multiple eukaryotic cellular and developmental processes and is linked with human diseases. Biol Chem 400, 1005–1022.
Li C, Furge KA, Cheng QC, Albright CF (2000). Byr4 localizes to spindle-pole bodies in a cell cycle-regulated manner to control Cdc7 localization and septation in fission yeast. J Biol Chem 275, 14381–14387.
Lizotte DL, Blakeslee JJ, Siryaporn A, Heath JT, DeLong A (2008). A PP2A active site mutant impedes growth and causes misregulation of native catalytic subunit expression. J Cell Biochem 103, 1309–1325.
Madeira F, Pearce M, Tivey ARN, Basutkar P, Lee J, Edbali O, Madhusoodanan N, Kolesnikov A, Lopez R (2022). Search and sequence analysis tools services from EMBL-EBI in 2022. Nucleic Acids Res 50, W276–W279.
Mangione MC, Gould KL (2019). Molecular form and function of the cytokinetic ring. J Cell Sci 132, jcs226928.
Minet M, Nurse P, Thuriaux P, Mitchison JM (1979). Uncontrolled septation in a cell division cycle mutant of the fission yeast Schizosaccharomyces pombe. J Bacteriol 137, 440–446.
Moreno S, Klar A, Nurse P (1991). Molecular genetic analysis of fission yeast *Schizosaccharomyces pombe*. Methods Enzymol 194, 795–823.
Morrell JL, Tomlin GC, Rajagopalan S, Venkatram S, Feoktistova AS, Tasto JJ, Mehta S, Jennings JL, Link A, Balasubramanian MK, Gould KL (2004). Sid4p-Cdc11p assembles the septation initiation network and its regulators at the S. pombe SPB. Curr Biol 14, 579–584.
Myles T, Schmidt K, Evans DR, Cron P, Hemmings BA (2001). Active-site mutations impairing the catalytic function of the catalytic subunit of human protein phosphatase 2A permit baculovirus-mediated overexpression in insect cells. Biochem J 357, 225–232.
Ogris E, Mudrak I, Mak E, Gibson D, Pallas DC (1999). Catalytically inactive protein phosphatase 2A can bind to polyomavirus middle tumor antigen and support complex formation with pp60(c-src). J Virol 73, 7390–7398.
Pollard TD (2010). Mechanics of cytokinesis in eukaryotes. Curr Opin Cell Biol 22, 50–56.
Ribeiro PS, Josue F, Wepf A, Wehr MC, Rinner O, Kelly G, Tapon N, Gstaiger M (2010). Combined functional genomic and proteomic approaches identify a PP2A complex as a negative regulator of Hippo signaling. Mol Cell 39, 521–534.
Rosenberg JA, Tomlin GC, McDonald WH, Snydsman BE, Muller EG, Yates JR, 3rd, Gould KL (2006). Ppc89 links multiple proteins, including the septation initiation network, to the core of the fission yeast spindle-pole body. Mol Biol Cell 17, 3793–3805.
Rothbauer U, Zolghadr K, Tillib S, Nowak D, Schermelleh L, Gahl A, Backmann N, Conrath K, Muyldermans S, Cardoso MC, Leonhardt H (2006). Targeting and tracing antigens in live cells with fluorescent nanobodies. Nat Methods 3, 887–889.
Rothbauer U, Zolghadr K, Muyldermans S, Schepers A, Cardoso MC, Leonhardt H (2008). A versatile nanotrap for biochemical and functional studies with fluorescent fusion proteins. Mol Cell Proteomics 7, 282–289.
Salimova E, Sohrmann M, Fournier N, Simanis V (2000). The *S. pombe* orthologue of the *S. cerevisiae mob1* gene is essential and functions in signalling the onset of septum formation. J Cell Sci 113, 1695–1704.
Schmidt S, Sohrmann M, Hofmann K, Woollard A, Simanis V (1997). The Spg1p GTPase is an essential, dosage-dependent inducer of septum formation in *Schizosaccharomyces pombe*. Genes Dev 11, 1519–1534.
Sievers F, Higgins DG (2021). The Clustal Omega Multiple Alignment Package. Methods Mol Biol 2231, 3–16.
Simanis V (2015). Pombe's thirteen - control of fission yeast cell division by the septation initiation network. J Cell Sci 128, 1465–1474.
Singh NS, Shao N, McLean JR, Sevugan M, Ren L, Chew TG, Bimbo A, Sharma R, Tang X, Gould KL, Balasubramanian MK (2011). SIN-Inhibitory Phosphatase Complex Promotes Cdc11p Dephosphorylation and Propagates SIN Asymmetry in Fission Yeast. Current biology: CB 21, 1968–1978.
Sohrmann M, Schmidt S, Hagan I, Simanis V (1998). Asymmetric segregation on spindle poles of the *Schizosaccharomyces pombe* septum-inducing protein kinase Cdc7p. Genes Dev 12, 84–94.
Sparks CA, Morphew M, McCollum D (1999). Sid2p, a spindle pole body kinase that regulates the onset of cytokinesis. J Cell Biol 146, 777–790.
Tang Y, Chen M, Zhou L, Ma J, Li Y, Zhang H, Shi Z, Xu Q, Zhang X, Gao Z, *et al*. (2019). Architecture, substructures, and dynamic assembly of STRIPAK complexes in Hippo signaling. Cell Discov 5, 3.
Wach A, Brachat A, Poehlmann R, Philippsen P (1994). New heterologous modules for classical or PCR-based gene disruptions in Saccharomyces cerevisiae. Yeast 10, 1793–1808.
Wachowicz P, Chasapi A, Krapp A, Cano Del Rosario E, Schmitter D, Sage D, Unser M, Xenarios I, Rougemont J, Simanis V (2015). Analysis of S. pombe SIN protein association to the SPB reveals two genetically separable states of the SIN. J Cell Sci 128, 741–754.
Xiao Y, Dong J (2021). The Hippo Signaling Pathway in Cancer: A Cell Cycle Perspective. Cancers (Basel) 13, 6241.
Zheng Y, Liu B, Wang L, Lei H, Pulgar Prieto KD, Pan D (2017). Homeostatic Control of Hpo/MST Kinase Activity through Autophosphorylation-Dependent Recruitment of the STRIPAK PP2A Phosphatase Complex. Cell Rep 21, 3612–3623.
Zhuo S, Clemens JC, Stone RL, Dixon JE (1994). Mutational analysis of a Ser/Thr phosphatase. Identification of residues important in phosphoesterase substrate binding and catalysis. J Biol Chem 269, 26234–26238.